Journal of Solid State Chemistry 181 (2008) 2386–2392

Contents lists available at ScienceDirect

Journal of Solid State Chemistry

journal homepage: www.elsevier.com/locate/jssc

Isomorphous substitution of europium for strontium in the structure of synthetic hydroxovanadate

E.I. Get'man [a], N.V. Yablochkova [a], S.N. Loboda [a], V.V. Prisedsky [b,*], V.P. Antonovich [c], N.A. Chivireva [c]

[a] Department of Inorganic Chemistry, Donetsk National University, 24 Universitetskaya, Donetsk 83055, Ukraine
[b] Department of General Chemistry, Donetsk National Technical University, 58 Artema, Donetsk 83000, Ukraine
[c] A.V. Bogatsky Physico-Chemical Institute, National Academy of Sciences, 86 Lustdorfskaya doroga, Odessa 65080, Ukraine

ARTICLE INFO

Article history:
Received 19 March 2008
Received in revised form
30 May 2008
Accepted 2 June 2008
Available online 5 June 2008

Keywords:
Isomorphism
Apatite
Hydroxovanadate
RE elements
Single-phase region
Structural and spectroscopic characteristics
Water absorbent

ABSTRACT

Polycrystalline strontium–europium hydroxovanadates $Sr_{10-x}Eu_x(VO_4)_6(OH)_{2-x}O_x$ were synthesized and studied by X-ray powder diffraction, infrared absorption and diffuse-reflectance spectroscopies and also thermogravimetry. The single-phase region of isomorphous substitution of Eu for Sr in hydroxovanadate has been found to lie in the compositional interval $0 \leqslant x \leqslant 0.18$ at 800 °C. Refinement of X-ray diffraction (XRD) patterns by the Rietveld method shows that Eu substitutes for Sr preferentially at the Sr(1) sites of the apatite structure. The substitution results in a more uniform distribution of Sr–O bond lengths in coordination polyhedra both around Sr (1) and Sr (2) sites and also in a slight contraction of the vanadate anion VO_4^{3-}. Synthetic Sr hydroxovanadates absorb a considerable amount of water in two forms: capillary condensed and chemically combined. The latter form may be absorbed at temperatures as high as 500 °C.

1. Introduction

The interest in isomorphism remains high in solid-state chemistry as the functional properties of many practically important materials may be modified by introduction of isomorphous additives to their structure. Compounds belonging to the apatite structure type accommodate a wide variety of isovalent and heterovalent substitutions, facilitating the efficiency of their application as biomaterials, catalysts, sensors, luminescent materials, sorbents, etc. [1–5].

Although the ability of vanadate ion to substitute for phosphate in calcium, strontium and lead apatites is well known, isomorphism in vanadate apatites has not been studied as thoroughly as in phosphates. Vanadate ions occupy crystallographic sites equivalent to PO_4^{3-} and the site symmetry of VO_4^{3-} ion in Ca and Sr vanadates is C_s—the same as that of PO_4^{3-} in phosphates [3–6]. At the same time, an increase of the site symmetry to C_{3v} and contraction of vanadate ions are observed in phosphate–vanadate solid solutions [6].

The substitution of rare-earth (RE) elements into apatites could result in their interesting applications as luminescent, laser materials and catalysts [4,5,7]. At present, little data are available on the limits of such substitutions in vanadate systems. Also, structural data on substituted vanadate apatites are not as complete as the data on phosphates. The study of the substitution of RE in single-crystalline Ca phosphate hydroxoapatites [7] showed that the uptake of RE, as measured by the crystal/melt partition coefficient, decreased from $x = 0.286$ to 0.212 through the series La, Nd, Sm, Dy, not counting a weak maximum ($x = 0.316$) at Nd. As well as in fluoroapatites, RE elements generally favored Ca(2) sites in phosphate hydroxoapatites, but the RE Ca(2)/Ca(1) site occupancy ratio decreased almost to unity in the lanthanide series.

In previous XRD studies [8–11], we found that the substitution limits, x_{max}, in hydroxovanadates $Sr_{10-x}RE_x(VO_4)_6(OH)_{2-x}O_x$ decreased in the lanthanide series from 0.40 for La to 0.07 for Gd. Rietveld refinements of powder XRD data showed that for Sr hydroxovanadates the RE Sr(2)/Sr(1) site occupancy ratio was less than unity, contrary to the above-mentioned results for Ca phosphate hydroxoapatites. That may be compared with the observed site occupancy ratios for chloroapatites which were generally less than unity and decreased to as low as 0.1 for Dy [23]. The substitution behavior may be controlled by complex combination of such factors as charge compensation, spatial accommodation of substituents, substitution mechanism and structural change in apatite, the volatile anion component [7].

To widen the list of previously studied elements in the first-half of the RE series, the heterovalent substitution of europium for strontium in the structure of synthetic strontium hydroxovanadate is studied in this work.

* Corresponding author.
E-mail address: prisedsky@feht.dgtu.donetsk.ua (V.V. Prisedsky).

0022-4596/$ - see front matter © 2008 Elsevier Inc. All rights reserved.
doi:10.1016/j.jssc.2008.06.003

2. Experimental

The starting chemicals used were $Sr(NO_3)_2$ ("pure for analysis"), Eu_2O_3 (EvO-Zh grade) and NH_4VO_3 ("chemically pure"). Weighed portions of starting reagents were taken to correspond to final composition $Sr_{10-x}Eu_x(VO_4)_6(OH)_{2-x}O_x$ ($0 \leqslant x \leqslant 0.80$) assuming the following scheme of substitution for strontium and hydroxide ions [8–11]:

$$Sr^{2+} + OH^- \rightarrow Eu^{3+} + O^{2-}.$$

Strontium–europium hydroxovanadates were synthesized from nitric–tartaric solutions. $Sr(NO_3)_2$ was dissolved in water, Eu_2O_3 in minimal quantity of concentrated nitric acid (about 1 mL per 1 g of weight), and NH_4VO_3 was dissolved in aqueous solution of tartaric acid. The solutions were mixed according to the stoichiometry and then evaporated. The dry residues obtained were ground in an agate mortar for 10–15 min and then calcined at 600–850 °C.

The samples of synthesized hydroxovanadates with various degrees of substitution were studied by X-ray powder diffraction, infrared (IR) spectroscopy, spectroscopy of diffuse reflectance and thermogravimetry.

The phase composition of synthesized samples was determined by then X-ray powder diffraction using a DRON-2 diffractometer at scanning rate 1–2°(2θ)/min using filtered (Ni) Cu$K\alpha$ radiation. To determine interplanar distances, powder diffraction patterns were recorded at scanning rate of 0.2–0.5(2θ)/min. The unit-cell parameters a and c were calculated by the least-square procedure taking into account the positions of 7 unambiguously indexed reflections in the range $40 < 2\theta < 50°$ (Si was used as an external standard).

To obtain data for crystal structure refinement, the patterns were scanned in steps of 2θ equal to 0.05°, in the range $15 \leqslant 2\theta \leqslant 140°$, at a counting time of 10 s/step. The data were analyzed using the Rietveld procedure [12] with the program FullProf.2k (version 2.80) from WinPLOTR package [13]. As starting data in these calculations, atomic coordinates in calcium hydroxoapatite as determined by Rietveld refinement of the structure from powder XRD data in [14] were used.

IR spectra were recorded in the wavenumber range from 400 to 4000 cm^{-1} with a Perkin-Elmer Spectrum BX spectrometer. The samples were pressed into pellets with KBr.

Spectra of diffuse reflectance were recorded with a Perkin-Elmer Lambda 9 UV/vis/NIR Spectrophotometer in the range of wavelength 200–2500 nm from samples placed in a Plexiglas cell with a quartz window. IR diffuse-reflectance spectroscopy has been used, in particular, to confirm the limits of the homogeneity region.

Thermal behavior of synthesized Sr–Eu hydroxovanadates was studied gravimetrically in an experimental setup described earlier [15]. A powdered sample in a Pt crucible was suspended with a Pt wire inside a vertical quartz tube in an electrical furnace with NiCr heaters. The weight of the sample during its heating up, holding at a given temperature and cooling down was recorded continuously by an electronic balance.

3. Results and their discussion

3.1. Homogeneity region from XRD data

According to XRD examinations, the phase composition of synthesized samples becomes stable after 80 h treatment at 800 °C. At lower temperatures, chemical interactions during synthesis proceed at insufficient rate, while at higher temperatures, noticeable thermal decomposition of hydroxovanadates occurs.

The samples in the compositional range $0 \leqslant x \leqslant 0.20$ are found to be single-phased strontium hydroxovanadates. In the XRD pattern for the sample with $x = 0.24$, well-defined reflections from strontium orthovanadate $Sr_3(VO_4)_2$ and europium oxide Eu_2O_3 are also seen. The intensities of these peaks grow with increasing the degree of substitution in the range $0.24 \leqslant x \leqslant 0.80$ indicating that these compositions lie in a multiphase region. No indication of any other crystal phase has been revealed by XRD.

The compositional dependences of hexagonal unit-cell parameters a and c within the hydroxovanadate single-phase region are shown in Fig. 1. The parameters were calculated from the positions of 7 distinct reflections in the range $40 < 2\theta < 50°$. Despite quite narrow limits in which the parameters change with x and also evident scattering, the linear fits of the data show a clear tendency of decrease in both a and c with increasing Eu content. Such behavior should be expected from the difference in ionic radii of Sr^{2+} (1.45 Å) and Eu^{3+} (1.26 Å) [16]. In the multiphase region, even higher scattering in the as-determined lattice parameters was observed due to the overlap of hydroxovanadate and orthovanadate peaks in the diffraction patterns.

Fig. 2 illustrates the refinement of the location of the single-phase region boundary using the "disappearing phase" method. The Eu_2O_3 (hkl 222) reflection intensity is plotted against the Eu content in the system. Extrapolation of this dependence to the intersection with the abscissa axis ($I = 0$) gives an estimation for the homogeneity region boundary—the limit of isomorphous substitution of Eu for Sr in hydroxovanadate apatite structure: $x_{max} = 0.18$.

This value can be compared with previously [8–11] established substitution limits for Eu analogs in the first-half of the RE element series (Table 1).

The substitution limit decreases monotonically with increasing the RE atomic number through the series. This is in apparent accordance with a control of substitution by spatial accommodation of RE substituents as the difference in ionic radii between strontium and RE, r(Sr)–r(RE), increases in the same direction. Study of the substitution of RE in single-crystalline phosphate apatites [7] showed that the uptake of RE also generally decreased through the lanthanide series but showed a weak maximum near Nd. No such maximum is observed in our data for polycrystalline Sr hydroxovanadate.

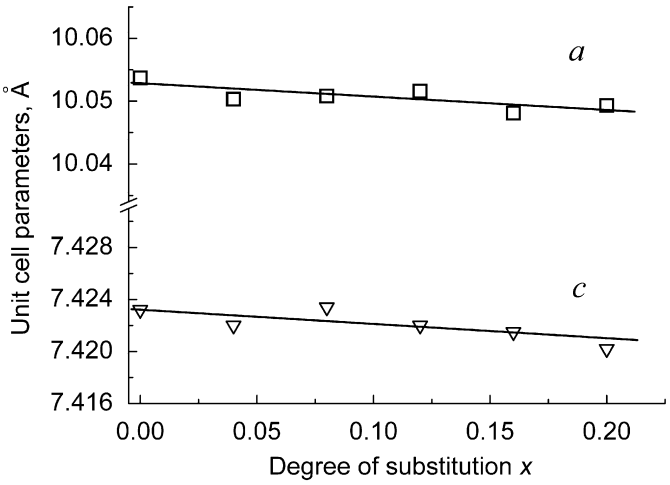

Fig. 1. Hexagonal unit-cell parameters a and c of $Sr_{10-x}Eu_x(VO_4)_6(OH)_{2-x}O_x$ in dependence on the degree of substitution.

3.2. IR spectroscopy

In Fig. 3, the IR absorption spectra recorded for the $x = 0$ and 0.20 samples are compared. The absorption band in the range from 650 to 950 cm^{-1} can be assigned to vibrations of the orthovanadate ion VO_4^{3-} [18]. The spectra display three maxima of absorption and are virtually similar for substituted ($x = 0.20$) and unsubstituted samples, except a visibly narrower peak at 815 cm^{-1} for the substituted sample.

Substitution of europium for strontium results in lower absorptions at 3570 and 560 cm^{-1} that correspond to stretching and librational modes of the hydroxide ion, respectively [17,18]. This observation supports the assumed scheme of isomorphous substitution: $Sr^{2+}+OH^- \rightarrow Eu^{3+}+O^{2-}$. Additional absorption at 580 cm^{-1} seen in the spectrum of the $x = 0.20$ solid solution can be assigned to a vibration of the Eu–O chemical bond [19].

The diffuse-reflectance spectra recorded both from Eu-substituted and -unsubstituted strontium hydroxovanadates display a broad absorption band in the near UV part of wavelengths in the range $200 \leqslant \lambda \leqslant 350$ nm. This absorption can be attributed to O $2p$–V $3d$ electron transitions in VO_4^{3-} tetrahedra [20]. The intensity and maximum position of this band show no clear dependence on the degree of substitution.

IR diffuse-reflectance spectroscopy has been also used to confirm the limit of substitution in strontium hydroxovanadate phase. For this purpose, diffuse-reflectance spectra recorded from $Sr_{10-x}Eu_x(VO_4)_6(OH)_{2-x}O_x$ samples are compared with the spectrum from Eu_2O_3 in Fig. 4.

Three characteristic peaks of absorption are observed in the near IR part of Eu_2O_3 spectrum at wavelengths 1990, 2070 and 2170 nm (Fig. 4a). They can be attributed to $^7F_{0,1} \rightarrow {}^7F_{5,6}$ electron transitions in 4f-subshell of Eu(III) atoms [21]. The density of Eu atoms in hydroxovanadates at studied degrees of Eu substitution is orders of magnitude lower than that in Eu_2O_3. Under these circumstances, a sharp increase of absorption at these bands in a spectrum indicates the appearance of Eu_2O_3 phase. The three bands are almost not visible in the spectrum taken from the $x = 0.16$ sample while they clearly reveal themselves in the spectrum for $x = 0.20$ (Fig. 4b). These data indicate that the $x = 0.20$ composition lies in the multiphase region (contrary to the data from less sensitive XRD patterns) while at $x = 0.16$ the sample is yet single-phased. Comparing these results with the extrapolation of the second-phase reflection intensity against the degree of europium substitution in Fig. 2, we can conclude that the homogeneity region of $Sr_{10-x}Eu_x(VO_4)_6(OH)_{2-x}O_x$ lies in the compositional interval $0 \leqslant x \leqslant 0.18$.

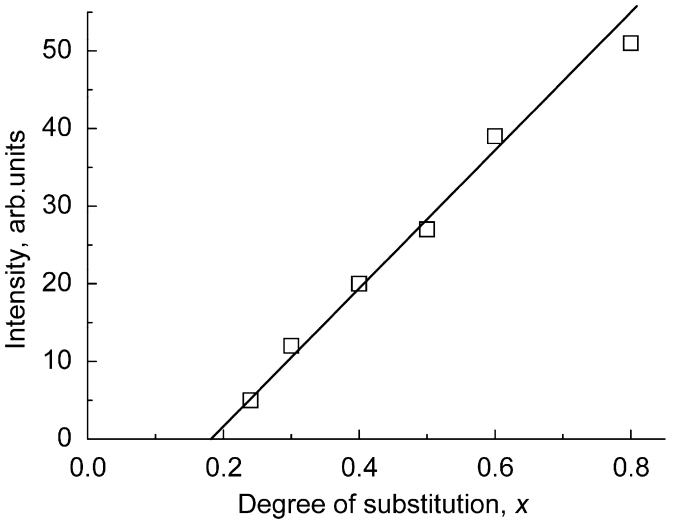

Fig. 2. Dependence of the Eu_2O_3 (*hkl* 222) reflection intensity on the degree of substitution.

Table 1
Substitution limits, x_{max}, for $Sr_{10-x}RE_x(VO_4)_6(OH)_{2-x}O_x$ and crystal radii of rare-earth substituents

RE substituent	La	Pr	Nd	Sm	Eu	Gd
x_{max}	0.40 [8]	0.28 [9]	0.28 [10]	0.24 [11]	0.18	0.07 [11]
Crystal radius (r) for 9-fold coordination (Å) [16]	1.36	1.32	1.30	1.27	1.26	1.25
r(Sr)–r(RE) (Å)	0.09	0.13	0.15	0.18	0.19	0.20

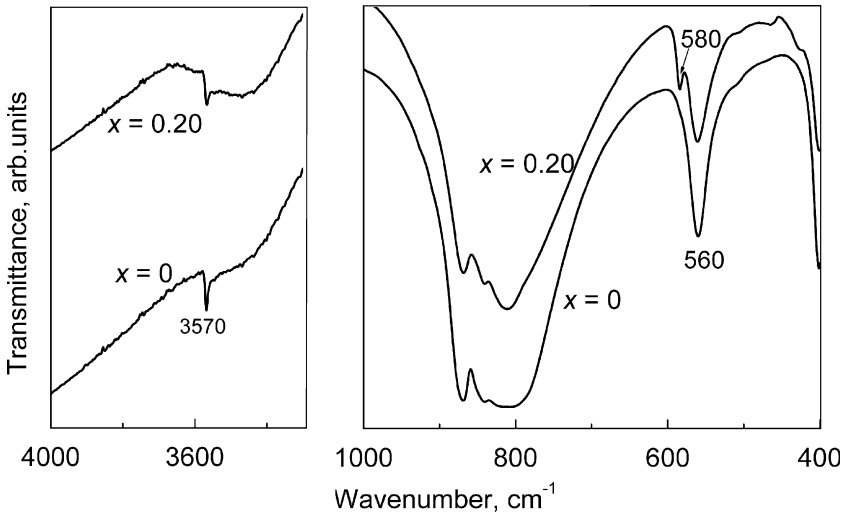

Fig. 3. IR spectra of $Sr_{10-x}Eu_x(VO_4)_6(OH)_{2-x}O_x$ samples.

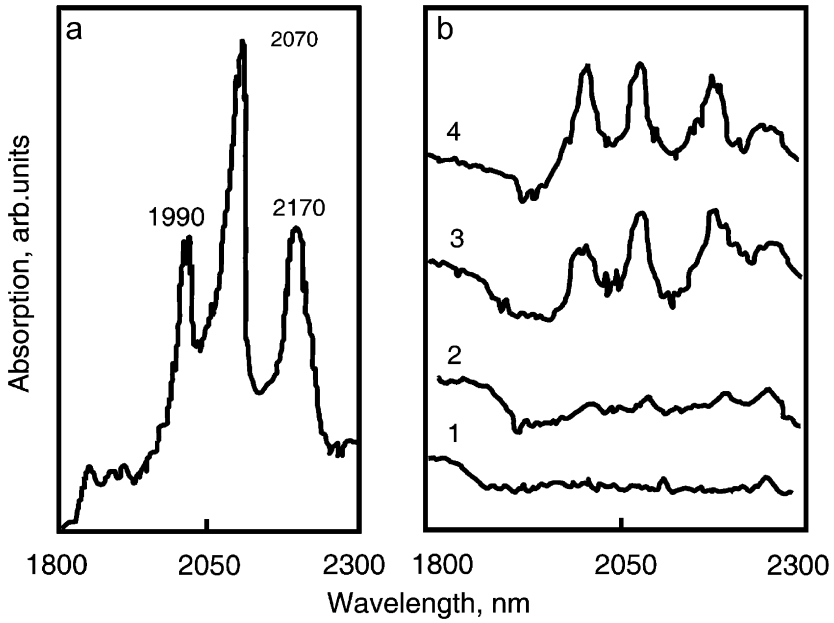

Fig. 4. Diffuse-reflectance spectra of Eu_2O_3 (a) and $Sr_{10-x}Eu_x(VO_4)_6(OH)_{2-x}O_x$ (*b*) for $x = 0$ (1), $x = 0.16$ (2), $x = 0.20$, (3) and $x = 0.24$ (4).

3.3. Rietveld structure refinement

The structural refinement of the $Sr_{10-x}Eu_x(VO_4)_6(OH)_{2-x}O_x$ vanadates for $x = 0$ and 0.20 was performed by the Rietveld method using $Ca_{10}(PO_4)_6(OH)_2$ as the starting model [14]. The final refinement data are presented in Table 2. Calculated reliability factors (*R*) confirm that the model provides an adequate fit for the collected XRD data.

The fractional atomic coordinates together with isotropic thermal parameters and site occupancies are given in Table 3. The data indicate that Eu^{3+} ions substitute for Sr^{2+} preferentially in Sr(1) sites of the apatite structure. The site occupancy ratio Eu–Sr(2)/Eu–Sr(1) is $0.011/0.033 = 0.33$ for the studied sample $Sr_{9.80}Eu_{0.20}(VO_4)_6(OH)_{1.80}O_{0.20}$.

The observed preference of Eu for the Sr(1) site could not be expected from simple considerations based on the substituent spatial accommodation ("the larger ions fill the larger sites"). Since Eu^{3+} is markedly smaller than Sr^{2+} (crystal radii for 7-fold coordination of 1.15 and 1.35 Å, respectively [16]), it may be anticipated to fill mainly the smaller Sr(2) sites. This is a fairly open site, where the nearest neighbor environment is formed from a hemisphere of six oxygens capped by the hydroxide anion. Minimization of the energy of electrostatic attraction between excess charges of Eu^{3+} and O^{2-}(4) would also provoke Eu^{3+} entering Sr(2) site. The strong preference of light RE elements for the Ca(2) position has been unchangeably confirmed for phosphate fluoro- and hydroxoapatites [7,22,23]. However, the Rietveld refinement of collected powder XRD data (Table 3) shows explicitly a strong preference of Eu^{3+} for the Sr(1) positions in hydroxovanadate.

Similar results for *RE*-site occupancy (*RE* = La, Pr, Nd) in hydroxovanadate were obtained in our previous studies [8–11] (Table 4). All the studied RE elements show a strong preference for sr(1) site, with the site occupancy ratio RE–Sr(2)/RE–Sr(1) varying from 0.06 for Pr to 0.33 for Eu. This ratio does not change uniformly through the light RE series La–Eu. No correlation can be found in the present data between the site occupancy ratio and the change in unit-cell volume or difference in ionic radii. The site occupancy ratio correlates negatively with the bond distance Sr(2)–OH (the correlation coefficient of −0.86) which is easily understood taking into account: (a) smaller ionic radius of Eu^{3+}; (b) stronger electrostatic attraction between Eu^{3+}(2) and OH^- or O^{2-}(4).

Table 2
Rietveld refinement for $Sr_{10-x}Eu_x(VO_4)_6(OH)_{2-x}O_x$

Phase		$Sr_{10-x}Eu_x(VO_4)_6(OH)_{2-x}O_x$	
		$x = 0$	$x = 0.20$
Space group		$P6_3/m$	
Structure type		Apatite	
Cell parameters (Å)	*a*	10.0544(3)	10.0418(5)
	c	7.4249(2)	7.4153(4)
Cell volume (Å^3)		650.03(3)	647.56(6)
Radiation, wavelengths λ_1 and λ_2 (Å)		CuKα 1.54056	1.54439
Angular range $2\theta_{min}$–$2\theta_{max}$ (deg)		15.000–140.000	
Number of measured reflections		960	799
Number of refinement parameters		37	41
Reliability factors	R_B	0.058	0.050
	R_F	0.052	0.051
	R_p	0.051	0.047
	R_{wp}	0.066	0.060
	χ^2	1.30	1.30

For comparison with phosphate apatites, it is interesting to note that, according to [7], the *RE*-site occupancy ratio *RE*–Ca(2)/*RE*–Ca(1) tends to increase asymptotically toward La in both F- and OH-phosphate apatites, and, in the opposite direction, it decreases almost to unity through the lanthanide series (i.e. with increasing difference in ionic radii, *r*(Ca)–*r*(RE)). Fleet et al. [7] suggested that in fluoro- and hydroxoapatites $Ca(1)O_9$ polyhedron does not readily accommodate cations that are either appreciably larger or appreciably smaller than Ca^{2+}. As $r(La^{3+})$ is only slightly larger than $r(Ca^{2+})$, they noted also that La behaves as though it is appreciably larger than other light RE ions. No such conclusion can be made for RE-substituted hydroxovanadates, as RE ions that favor Sr(1) positions are substantially smaller than Sr^{2+} (Table 4).

Table 3
Atomic coordinates (x, y, z), isotropic thermal parameters (B_{iso}) and crystallographic site occupancies (G) for $Sr_{10-x}Eu_x(VO_4)_6(OH)_{2-x}O_x$

Atom (site)	Crystallogr. position	Parameters	$Sr_{10-x}Eu_x(VO_4)_6(OH)_{2-x}O_x$	
			$x = 0$	$x = 0.20$
Sr(1)	4*f*	*X*	2/3	2/3
		Y	1/3	1/3
		Z	0.0016(9)	0.001(1)
		B_{iso} (Å^2)	0.85(8)	1.1(1)
		G	1	0.967(9)
Eu(1)	4*f*	*X*	–	2/3
		Y		1/3
		Z		0.001(1)
		B_{iso} (Å^2)		1.1(1)
		G		0.033(9)
Sr(2)	6*h*	*x*	0.2435(3)	0.2440(4)
		y	0.9888(4)	0.9887(5)
		z	1/4	1/4
		B_{iso} (Å^2)	0.80(6)	0.84(9)
		G	1	0.989(6)
Eu(2)	6*h*	*x*	–	0.2440(4)
		y		0.9887(5)
		z		1/4
		B_{iso} (Å^2)		0.84(9)
		G		0.011(6)
V	6*h*	*x*	0.3984(6)	0.3989(8)
		y	0.3672(6)	0.3675(8)
		z	1/4	1/4
		B_{iso} (Å^2)	0.47(13)	1.0(2)
		G	1	1
O(1)	6*h*	*x*	0.318(2)	0.323(2)
		y	0.482(2)	0.481(2)
		z	1/4	1/4
		B_{iso} (Å^2)	1.7(5)	1.7(6)
		G	1	1
O(2)	6*h*	*x*	0.592(2)	0.591(3)
		y	0.468(2)	0.464(2)
		z	1/4	1/4
		B_{iso} (Å^2)	0.7(4)	1.3(6)
		G	1	1
O(3)	12*i*	*x*	0.346(1)	0.345(2)
		y	0.253(1)	0.253(2)
		z	0.063(1)	0.065(2)
		B_{iso} (Å^2)	2.1(3)	2.0(4)
		G	1	1
OH	4*e*	*x*	0	0
		y	0	0
		z	0.198(4)	0.192(5)
		B_{iso}, Å^2	1.6(10)	3.7(9)
		G	0.5	0.45
O(4)	4*e*	*x*	–	0
		y		0
		z		0.193(5)
		B_{iso} (Å^2)		3.7(9)
		G		0.05

Table 4
RE site preference in hydroxovanadates $Sr_{10-x}RE_x(VO_4)_6(OH)_{2-x}O_x$

RE element	La [8]	Pr [9]	Nd [10]	Eu
Degree of substitution, x	0.36	0.28	0.28	0.20
Sr(1) site occupancy				
Sr	0.932	0.936	0.943	0.967
RE	0.069	0.064	0.057	0.033
Sr(2) site occupancy				
Sr	0.986	0.996	0.991	0.989
RE	0.014	0.004	0.009	0.011
Site occupancy ratio RE–Sr(2)/RE–Sr(1)	0.20	0.06	0.16	0.33
r(Sr)–r(RE) (%)	6.2	9.0	10.3	13.1
$\Delta V_{unit\text{-}cell}$ (Å^3)	−0.13	−2.32	−0.49	−2.47
Bond distance Sr(2)–OH (Å)	2.592	2.595	2.597	2.544

The comparison of our data with results [7] demonstrates that an increase in difference between $r(Ca^{2+}, Sr^{2+})$ and $r(RE^{3+})$ generally favors the preference of RE substituents for the Ca(1) site in the apatite structure. This follows from the observed change of the site occupancy ratio through the RE series [7] and from the observed strong preference of RE to the Sr(1) position in Sr hydroxovanadate (where the difference between $r(Sr^{2+})$ and $r(RE^{3+})$ is much greater than in Ca apatites), albeit the fact that a uniform decrease in the site occupancy ratio is not traced through the RE series in our data.

Interatomic distances calculated from the observed cell parameters and atomic coordinates are compared for substituted and unsubstituted hydroxovanadates in Table 5. Although the degree of substitution is not high (at $x = 0.20$ only 2 percent of Sr^{2+} ions are substituted by Eu^{3+}), appreciable changes in bond distances are evident.

As a result of substitution, the mean Sr(1)–O distance decreases from 2.725 to 2.714 Å, whereas the mean distance Sr(2)–O does not change noticeably. That is in accordance with a straightforward interpretation of the fact that the smaller Eu^{3+} ions enter preferentially Sr(1) positions.

At the same time, the particular distances between Sr ions both at (1) and (2) crystallographic sites and oxygens at different (1,2,3) sites change in a far more complicated way. The longer of these distances, such as Sr(1)–O(3), Sr(1)–O(2), Sr(2)–O(1), and Sr(2)–O(3), shorten in substituted hydroxovanadate, while shorter of them, such as Sr(1)–O(1), Sr(2)–O(2), and part of Sr(2)–O(3), elongate after substitution. As a result, a more uniform distribution of Sr–O bond lengths both in Sr(1) and Sr(2) coordination polyhedra arises in a substituted sample.

A straightforward interpretation may also be given to the observed decrease in bond distances Sr(2)–OH from 2.620 to 2.544 Å and Sr(2)–Sr(2) from 4.381 to 4.345 Å. This may be attributed to (a) partial substitution of a smaller Eu^{3+} ion for Sr^{2+}(2). (b) Increased electric charge of Eu^{3+} at Sr(2) site, (c) substitution of oxygen ion O^{2-} for hydroxide OH^- in the channels of the apatite structure as a result of charge compensation and its increased electrostatic attraction with neighboring Eu^{3+}(2) and Sr^{2+}(2) cations.

A slight contraction of vanadate anions may be noticed in the substituted sample: all the distances V–O(1), V–O(2) and V–O(3) become shorter and the mean distance ⟨V–O⟩; shortens from 1.720 to 1.680 Å. This observation looks rather unexpected taking into account a low degree of substitution and smaller size of

Table 5
Selected interatomic distances in $Sr_{10-x}Eu_x(VO_4)_6(OH)_{2-x}O_x$

	Interatomic distances (Å) for substitution degree x	
	$x = 0$	$x = 0.20$
V–O(1)	**1.700(18)**	**1.660(30)**
V–O(2)	1.719(18)	1.670(30)
V–O(3) × 2	1.731(9)	1.694(15)
⟨*V–O*⟩	*1.720*	1.680
Sr(1)–O(1) × 3	**2.559(14)**	**2.598(17)**
Sr(1)–O(2) × 3	2.628(12)	2.591(13)
Sr(1)–O(3) × 3	2.989(10)	2.953(12)
⟨*Sr(1)–O(1,2,3)*⟩	*2.725*	2.714
Sr(2)–O(1)	**2.832(16)**	**2.800(20)**
Sr(2)–O(2)	2.476(17)	2.540(30)
Sr(2)–O(3) × 2	2.824(9)	2.694(15)
Sr(2)–O(3) × 2	2.379(9)	2.490(15)
⟨*Sr(2)–O(1,2,3)*⟩	*2.619*	2.618
Sr(2)–OH	2.620(6)	2.544(8)
Sr(2)–Sr(2)	4.381(5)	4.345(5)

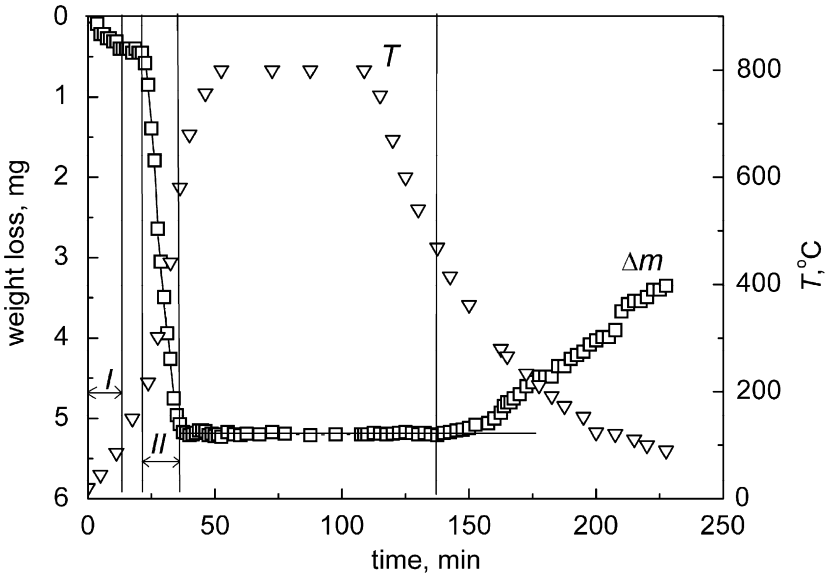

Fig. 5. Changes in the mass of $Sr_{10}(VO_4)_6(OH)_2$ sample ($m_0 = 1.0947$ g) in the heating–cooling cycle.

substituting ion, but a similar effect has also been observed for La, Pr, Nd and Sm substitutions [8–11].

From the data available at present, the substitution behavior of RE in hydroxovanadates is controlled by charge compensation and spatial accommodation of substituents, but it is felt that a more complex combination of crystal and stereochemical factors may contribute to the uptake and site preference of RE elements as well.

3.4. Thermal behavior of the samples

The ability of hydroxovanadates to absorb molecules at their surface is important in their application as sorbents or catalysts. To examine this ability of Sr hydroxovanadate, thermal behavior of both unsubstituted $Sr_{10}(VO_4)_6(OH)_2$ and substituted $Sr_{9,84}Eu_{0,16}(VO_4)_6(OH)_{1,84}O_{0,16}$ samples has been studied gravimetrically in the temperature range $20 < t < 800\,^{\circ}C$. Powdered samples about 1 g in mass were placed in a Pt crucible and heated up to 800 °C at an average rate of ~12 °C/min, held at this temperature for an hour, and then cooled down again to room temperature with the furnace. Weight loss (or gain) and temperature near the sample were monitored continuously during a heating–cooling cycle (Fig. 5).

The results of thermogravimetric studies do not depend on the degree of substitution of a sample, they are virtually identical for substituted and unsubstituted hydroxovanadates. Weight loss at heating goes on in two distinct stages, whereas weight gain during cooling is observed below 500 °C and continues more slowly (Fig. 5). After storing the sample for a day at room temperature in air, the initial weight is restored and does not change during further storage for 5 or more days.

From these facts and literature data, the observed changes in weight may be connected to the change of water content in the sample. Studies of water absorption on hydroxoapatites by means of NMR spectroscopy [1] have shown that H_2O molecules are connected to oxygen or hydroxide ions at the sample's surface by hydrogen bond and also capillary condensed water in micropores is present.

At stage I (Fig. 5), $20 < t < 110\,^{\circ}C$, total weight loss in the studied sample corresponds to the removal of 0.04 mole of water per mole of hydroxovanadate. In this temperature range, water condensed in micropores is evaporated.

At stage II, $200 < t < 600\,^{\circ}C$, much greater amount of water, 0.41 mol H_2O/mol $Sr_{10}(VO_4)_6(OH)_2$, is removed. Further heating from 600 to 800 °C does not change the weight indicating that all water has been lost from the sample. We may conclude that the major part of absorbed water, more than 90 percent, is chemically bonded on the surface of hydroxovanadate.

4. Conclusion

Strontium–europium hydroxovanadates $Sr_{10-x}Eu_x(VO_4)_6(OH)_{2-x}O_x$ were synthesized by evaporating the stoichiometric Sr, V, Eu nitric–tartaric solutions and calcining obtained residues at 800 °C for 80 h. According to XRD and diffuse-reflectance spectroscopy, the single-phase region of isomorphous substitution of Eu for Sr in the hydroxovanadate apatite structure lies in the interval $0 \leqslant x \leqslant 0.18$ at 800 °C. Refinements of XRD patterns by the Rietveld method show that Eu substitutes Sr predominantly at the Sr(1) sites of the apatite structure. The substitution brings about a more uniform distribution of Sr–O bond lengths in coordination polyhedra both for Sr (1) and Sr (2) sites and also a slight contraction of vanadate anion VO_4^{3-}. Synthetic Sr hydroxovanadates absorb a considerable amount of water in two forms: chemically bonded (about 0.4 mol H_2O/mol in the studied samples) and capillary condensed (~0.04 mol H_2O/mol). The former may be absorbed at temperatures as high as 500 °C.

References

[1] T. Kanazawa, Inorganic Phosphate Materials, Elsevier, Amsterdam, 1989, 298pp.
[2] Y. Liu, P. Comodi, Mineral. Mag. 57 (1993) 709–719.
[3] T. Hara, S. Kanai, K. Mori, et al., J. Org. Chem. 71 (2006) 7455–7462.
[4] L.D. DeLoach, S.A. Payne, B.H.T. Chai, G. Loutts, Appl. Phys. Lett. 65 (10) (1994) 1208–1210.
[5] O. Chukova, S. Nedilko, Z. Moroz, M. Pashkovskiy, J. Lumin. 102–103 (2003) 498–503.
[6] C.B. Boechat, J.-G. Eon, A.M. Rossi, C.A. de Castro Perez, R.A. da Silva San Gil, Phys. Chem. Chem. Phys. 2 (2000) 4225–4230.
[7] M.E. Fleet, X. Liu, Y. Pan, J. Solid State Chem. 149 (2000) 391–398.
[8] E.I. Get'man, V.I. Marchenko, S.N. Loboda, N.V. Grytsenko, Vestnik DonNU. Series A (1–2) (2005) 279–283 (in Russian).

[9] E.I. Get'man, V.I. Marchenko, S.N. Loboda, N.V. Yablochkova, Ukr. Chem. J. 73 (7) (2007) 6–9 (in Russian).
[10] E.I. Get'man, V.I. Marchenko, S.N. Loboda, N.V. Yablochkova, Russ. J. Inorg. Chem. 52 (2007) 187–189 (in Russian).
[11] E.I. Get'man, V.I. Marchenko, S.N. Loboda, N.V. Yablochkova, A.L. Plehov, Funct. Mater. (Ukraine) 14 (3) (2007) 317–320.
[12] H.M. Rietveld, J. Appl. Crystallogr. 15 (1982) 430.
[13] T. Roisnel, J. Rodriguez-Carvayal, in: Proceedings of the Seventh European Powder Diffraction Conference (EPDIC 7), Barcelona, 2000, pp. 118–123.
[14] R.M. Wilson, J.C. Elliot, S.E.P. Dowker, Am. Mineral. 84 (1999) 1406–1414.
[15] V.V. Prisedsky, V.M. Vinogradov, J. Solid State Chem. 177 (2004) 4258–4268.
[16] R. Shannon, Acta Crystallogr. A 32 (1976) 751–767.
[17] G. Engel, W.E. Klee, J. Solid State Chem. 5 (1972) 28–34.
[18] I.I. Plusnina, Infrared Spectra of Minerals, Moscow State University, Moscow, 1976, 175pp. (in Russian).
[19] A. Taitai, J.L. Lacout, J. Phys. Chem. Solids 7 (48) (1987) 629–633.
[20] A.A. Fotiev, B.V. Slobodin, M.Ya. Khodos, Vanadates: Composition, Synthesis, Structure and Properties, Nauka, Moscow, 1988, 270pp. (in Russian).
[21] W.B. White, Appl. Spectrosc. 3 (21) (1967) 171–176.
[22] A. Serret, M.V. Cabanas, M. Vallet-Regi, Chem. Mater. 12 (2000) 3836–3841.
[23] M.E. Fleet, X. Liu, Am. Mineral. 85 (2000) 1437–1446.